MOLECULAR NUCLEAR IMAGING FOR TARGETING AND TRAFFICKING

HEE-SEUNG BOM[1*], JUNG-JUN MIN[1] and HWAN-JEONG JEONG[2]
Department of Nuclear Medicine, Chonnam National University Hwasun Hospital
160 Ilshimri, Hwasun, Jeonnam, 519-609, Korea
[1]Department of Nuclear Medicine, Chonnam National University Medical School, Gwangju, Korea
[2]Department of Nuclear Medicine, Chonbuk National University Medical School, Jeongju, Korea
*Corresponding author. E-mail : hsbom@jnu.ac.kr

Received January 2, 2006

Noninvasive molecular targeting in living subjects is highly demanded for better understanding of such diverse topics as the efficient delivery of drugs, genes, or radionuclides for the diagnosis or treatment of diseases. Progress in molecular biology, genetic engineering and polymer chemistry provides various tools to target molecules and cells *in vivo*. We used chitosan as a polymer, and ^{99m}Tc as a radionuclide. We developed ^{99m}Tc-galactosylated chitosan to target asialoglycoprotein receptors for nuclear imaging. We also developed ^{99m}Tc-HYNIC-chitosan-transferrin to target inflammatory cells, which was more effective than ^{67}Ga-citrate for imaging inflammatory lesions. For an effective delivery of molecules, a longer circulation time is needed. We found that around 10% PEGylation was most effective to prolong the circulation time of liposomes for nuclear imaging of ^{99m}Tc-HMPAO-labeled liposomes in rats. Using various characteristics of molecules, we can deliver drugs into targets more effectively. We found that ^{99m}Tc-labeled biodegradable pullulan-derivatives are retained in tumor tissue in response to extracellular ion-strength. For the trafficking of various cells or bacteria in an intact animal, we used optical imaging techniques or radiolabeled cells. We monitored tumor-targeting bacteria by bioluminescent imaging techniques, dentritic cells by radiolabeling and neuronal stem cells by sodium-iodide symporter reporter gene imaging. In summary, we introduced recent achievements of molecular nuclear imaging technologies in targeting receptors for hepatocyte or inflammatory cells and in trafficking bacterial, immune and stem cells using molecular nuclear imaging techniques.

KEYWORDS : Molecular Imaging, Nuclear Medicine, Polymer, Targeting, Trafficking, Stem Cell, Tumor

1. INTRODUCTION

Noninvasive molecular targeting in living subjects is highly demanded for efficient delivery of drugs, genes, or radionuclides in the course of diagnosing or treating diseases. Nuclear medicine has been used for decades to evaluate *in vivo* biochemistry using organ- or cell-specific radiopharmaceuticals such as ^{131}iodine for thyroid follicular cells. Recent progress in molecular biology provides tools for unveiling secrets of intra- or inter-cellular events including gene transfer. Molecular nuclear imaging uses those tools to trace molecular events in living animals or in the human. Molecular biology also has produced advanced cell therapy technologies. Stem cells are expected to treat various otherwise incurable diseases. For a proper selection of time and number of cells, trafficking of administered cells is needed. Molecular nuclear imaging technology using luminescent or radioactive photons is most suitable for the purpose. Fig. 1 illustrates the concept of targeting and trafficking.

2. METHODS AND RESULTS IN NUCLEAR IMAGING EXPERIMENTS OF TARGETING AND TRAFFICKING

2.1 Hepatocyte-Targeted Nuclear Imaging Using ^{99m}Tc-Galactosylated Chitosan

For this field, we developed a hepatocyte-targeted nuclear imaging agent using chitosan. Asialoglycoprotein receptors (ASGP-R) that specifically exist on the surface of mammalian polygonal cell of liver. As ASGP-R recognize galactose or N-acetylgalactosamine residues of desialylated glycoproteins, materials having these ligands, regardless of whether or not a monomer or a polymer, have been studied for targeting hepatocytes directly. Here, the target molecule is the asialoglycoprotein receptor and the ligand to be used is galactose of lactobionic acid. For acquiring nuclear gamma images, the pharmaceutical should chelate with a radionuclide such as ^{99m}Tc. Because galactosylated chitosan (GC) is weakly chelated to ^{99m}Tc, we used galactosyl-methylated

chitosan (GMC) which is chemically modified to improve labeling efficiency with ^{99m}Tc [1]. The radiolabeling efficiency of ^{99m}Tc-GC *in vitro* and in serum was 95% by incorporation of methyl groups, which lasted up to 6 hours. After GMC was labeled with ^{99m}Tc, the possibility of liver-targeted nuclear imaging was investigated. The gamma-camera images showed rapid localization of ^{99m}Tc-GMC to liver. In contrast, galactose-free ^{99m}Tc-MC accumulated faintly in the liver (Fig. 2). GMC-labeled fluorescein isothiocyanate (FITC-GMC) was primarily positioned in hepatocytes but not in Kupffer cells. Therefore, we concluded that ^{99m}Tc-GMC specifically localized to the liver, as targeting the ASGP-R on the hepatocyte. Recently, we also developed the other form of galactosylated chitosan, hydrazinonicotinamide-galactosylated chitosan (HGC), to stabilize the high labeling efficiency without methylation of chitosan. To demonstrate that liver uptake of ^{99m}Tc-HGC occurred by means of the ASGP-R mediated process, two mice were co-injected with free galactose. The result of this inhibition study showed that hepatic uptake of ^{99m}Tc-HGC was blocked by the co-

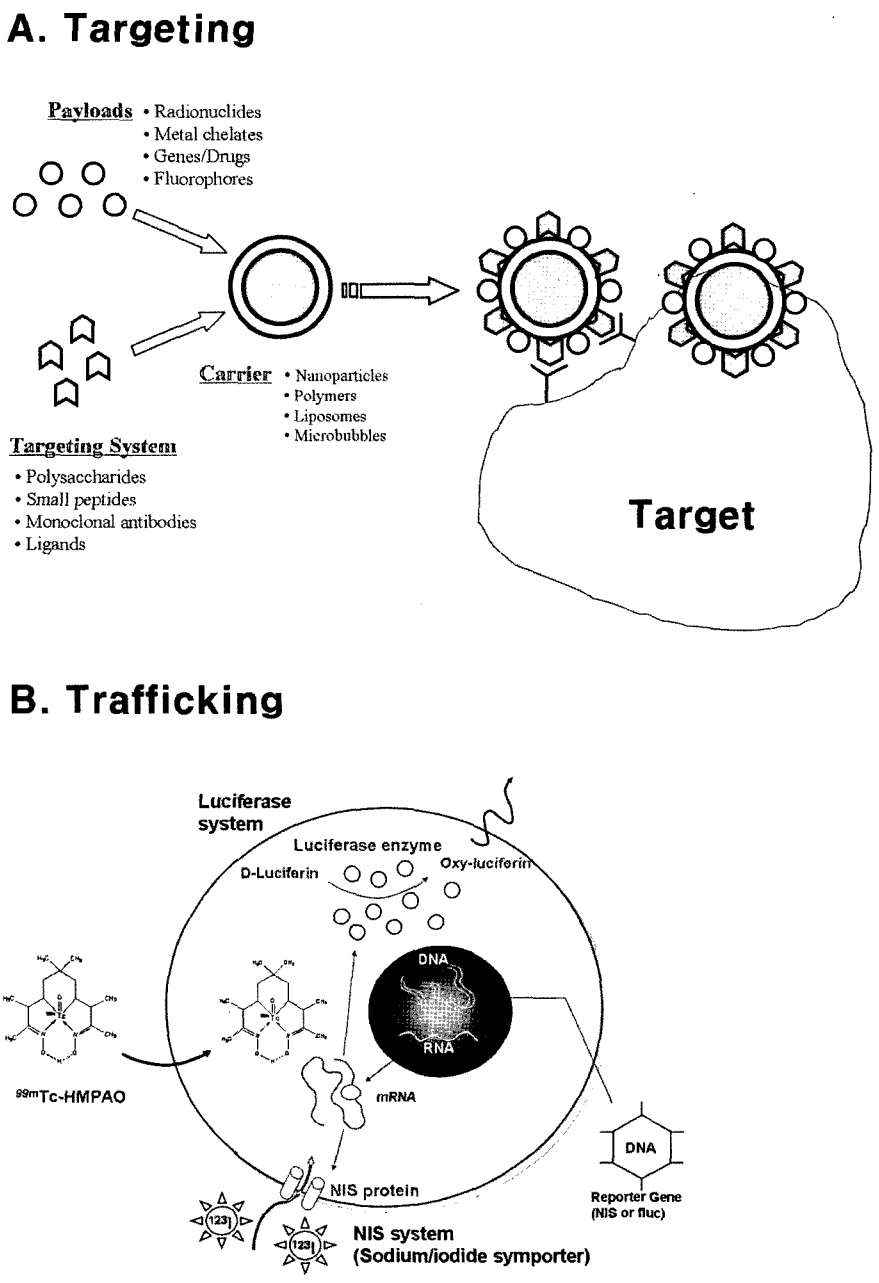

Fig. 1. Concept of Molecular Targeting and Trafficking Using Nuclear Medicine Techniques

injection of free galactose. In conclusion, ^{99m}Tc-HGC showed specific and rapid targeting to hepatocytes. It is a promising receptor-specific radiopharmaceutical with potential applications in liver imaging for evaluation of hepatocytic function.

3. TARGETING TUMOR AND INFLAMMATORY LESIONS USING LIPOSOMES AND POLYMERS

3.1 Polyethyleneimine-Derivatives to Target Transferring Receptors in Tumor an Inflammatory Cells

Polyethyleneimine (PEI) has been extensively investigated for use as a nonviral gene delivery vector due to its "proton sponge" mechanism. To overcome nonspecific interactions between blood components and cationic delivery system, various nonionic water-soluble polymers have been introduced [i.e., poly(ethylene glycol) (PEG), poly (N-vinyl-pyrrolidone) (PVP), poly[N-(2-hydroxypropyl) methacrylamide] (PHPMA), etc]. We applied the nuclear imaging technique to monitor the effect of PEGylation of PEI delivery system *in vivo*. PEI exhibits a high positive charge density in aqueous solution. It contains primary, secondary and tertiary amino groups. Due to these properties, PEI polymer could become complex with a reduced amount of ^{99m}Tc. We synthesized galactosylated PEI-PEG with different levels of PEG substitution ranging from 4.1 to 13.3 mol% of PEI amino groups. Validation of the differences of the *in vivo* distribution in various degrees of PEG substitution was performed using nuclear imaging with a gamma camera. After systemic administration of ^{99m}Tc-PEGylated Gal-PEIs, rapid accumulation in the liver, spleen and lungs was observed. With increasing amounts of PEG, the lung uptake was markedly reduced. These results demonstrate that nuclear imaging technique may be used as a basic screening tool for determining the optimized system of PEGylated Gal-PEIs [2]. As to applying these results to gene complexes, we made ^{99m}Tc labeled GPP_{50}/DNA complexes which were injected into the mice via the tail vein. Gamma images were then acquired at 5, 15 and 30 min. We confirmed that the gamma images resulting from the ^{99m}Tc labeled complexes help predict the in vivo biodistribution of the gene complexes [3].

3.2 Polyethylene Glycol (PEG) Modified ^{99m}Tc-HMPAO-Liposome for Improving Blood Circulation and Biodistribution: The Effect of the PEGylation Extent [4]

Modification of liposomes using polyethylene glycol (PEG) results in steric hindrance and prolongation of blood circulation time. This characteristic of PEG, however, can reduce radiolabeling efficiency (RE) when using the glutathione method for the radiolabeling liposomes. Therefore, we investigated the effect of PEGylation extent (PEGExt: 0, 5, 9.6 and 13.7 mol%) on the *in vivo* biodistribution of liposomes in Wistar rats, and RE with ^{99m}Tc. PEGylated liposomes were prepared with egg PC (1.85 mol%), cholesterol (1.0 mol%) and DSPE-PEG2000 (0, 5, 9.6 and 13.7 mol%, respectively). The size distribution of the PEGylated liposomes was analyzed by dynamic light scattering. The ^{99m}Tc-HMPAO complexes were used for radiolabeling of preformed liposomes. The labeling efficiency and stability were analyzed with a Sephadex G-15 column, and the

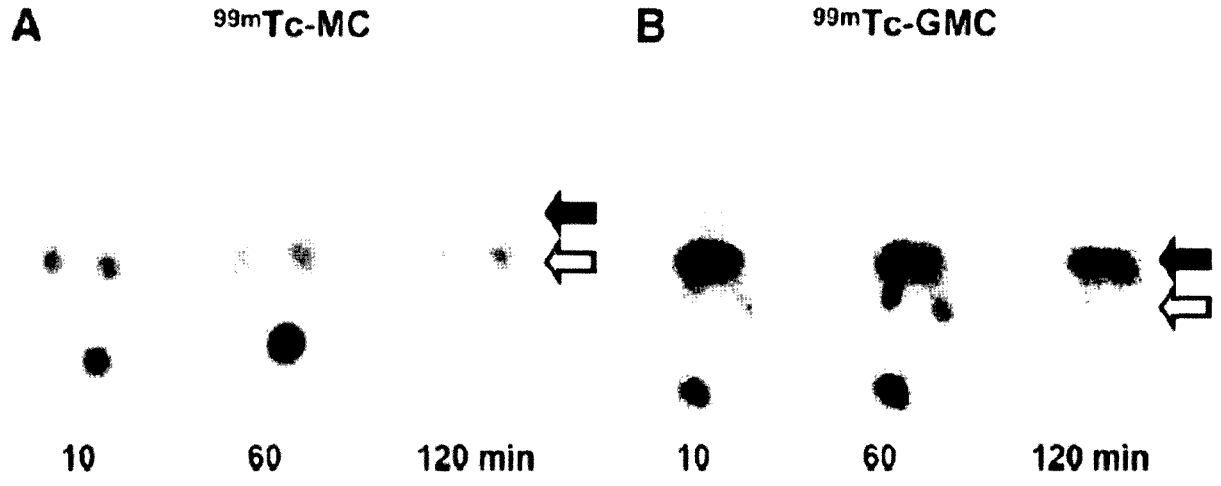

Fig. 2. Gamma Camera Images of Mice at 10, 60 and 120 min after Injection of ^{99m}Tc-MC (A) and ^{99m}Tc-GMC (B). After ^{99m}Tc-GMC Injection into mice, ^{99m}Tc-GMC was Specifically Localized to Liver (B), but ^{99m}Tc-MC Uptake was Faint (A). Solid Arrows Point to Liver; Open Arrows Indicate Kidneys of Each Animal

biodistribution studies of ^{99m}Tc-liposomes after intravenous injection was also investigated in Wistar rats. The sizes of PEGylated liposomes decreased by increasing the PEGExt to 9.6 mol%, whereas sizes increased at 13.7 mol%. RE of ^{99m}Tc were greater than 90% for all PEGExt tested, and radiolabeling stability in human plasma was enhanced as a function of PEGExt. Liposomes without PEG were cleared rapidly from blood and accumulated preferentially in the liver and the spleen. When PEGExt was increased, the accumulation in the organs decreased. This accumulation of PEG was maximized at 9.6 mol%. Accumulation of the liposomes in the spleen was increased again when PEGExt increased to 13.7 mol%. The splenic uptake of liposomes seemed to be dependant not only on PEGExt but also on the size of the liposomes. In conclusion, the PEG chains on the surface of liposome had no influence on the labeling efficiency, and the effect of PEG on the prolongation of circulation time was maximized at 9.6 mol% PEG.

3.3 ^{99m}Tc-HYNIC-Chitosan-Transferrin as an Imaging Agent of Infectious Foci [5]

Transferrin is a key molecule in ^{67}Ga-citrate scintigraphy. We synthesized ^{99m}Tc-labeled transferrin and compared it with ^{67}Ga-citrate for detection of infectious foci. Succunimidyl 6-hydrazino nicotinate hydrochloride (HYNIC)-chitosan-transferrin was synthesized and radiolabeled with ^{99m}Tc. Labeling efficiencies of ^{99m}Tc-HYNIC-chitosan-transferrin (^{99m}Tc-transferrin) were determined at 10 and 30 min, 1, 2, 4 and 8 hr. Biodistribution and imaging studies with ^{99m}Tc-transferrin and ^{67}Ga-citrate were performed in a rat abscess model induced with approximately 2×10^8 colony forming units of *Staphylococcus aureus* ATCC 25923 in 0.2 ml of bacterial suspension. Successful synthesis of HYNIC-chitosan-transferrin conjugate was confirmed by mass spectrometry. Labeling efficiencies of ^{99m}Tc-transferrin were 96.2±0.7%, 96.4±0.5%, 96.6±1.0%, 96.9±0.5%, 97.0±0.7% and 95.5±0.7% at 10 and 30 min, 1, 2, 4 and 8 hr, respectively. The injected doses per gram tissue (%ID/g) of ^{99m}Tc-transferrin were 0.18±0.01 and 0.18±0.01 in the lesions and 0.05±0.01 and 0.04±0.01 in normal muscle at 30 min and 3 hr: Lesion-to-normal muscle uptake ratios were 3.7±0.6 and 4.7±0.4 at 30 min and 3 hr, respectively. On scintigraphic images, lesion-to-background ratios of ^{99m}Tc-transferrin were 2.18±0.03, 2.56±0.11, 3.08±0.18, 3.77±0.17, 4.70±0.45 and 5.59±0.40 at 10 and 30 min, 1, 2, 4 and 10 hr, and those of ^{67}Ga-citrate were 3.06±0.84, 4.12±0.54 and 4.55±0.74 at 2, 24 and 48 hr, respectively. ^{99m}Tc-transferrin had higher and more rapidly increased uptake in the lesions compared to ^{67}Ga-citrate. In conclusion, transferrin can be labeled with ^{99m}Tc. Labeling efficiencies of ^{99m}Tc-transferrin were higher than 95%, and radiolabeling was stable for at least 8 hours. ^{99m}Tc-transferrin scintigraphy showed higher image quality in shorter time compared to ^{67}Ga-citrate image.

3.4 Biodegradable Nano-Sized Pullulan Derivatives for Tumor-Targeted Delivery of Radioisotopes [6]

Nanoparticles of pullulan derivatives (PD) are self-assembled hydrogel nanoparticles which are responsive to extracellular pH. We evaluated the potential of PD as a tumor-targeting carrier of radioisotope. Four types of PD: pullulan acetate (PA), succinylated PA (SPA), PA-DTPA and SPA-DTPA conjugates were prepared. They were radiolabeled with ^{99m}Tc. Labeling efficiencies were determined at 30 min, 1, 2, 4 and 12 hours. CT-26 colon cancer cells were subcutaneously injected into Balb/c mice. After 2 weeks of subcutaneous injection of CT-26 cells, Tc-99m-labeled PD (Tc-PD) were injected into the tumors. Whole body images of mice were obtained at 30 min, 1, 2, 4 and 12 hours after intratumoral injection. Labeling efficiencies of PA, PA-DTPA, SPA and SPA-DTPA were 94.5±5.9%, 97.8±3.5%, 94.2±3.8%, and 92.5±6.2%, respectively ($p > 0.05$). The percent retention rates of these preparations were not different, but were significantly higher than that of Tc-99m pertechnetate. In conclusion, the pH-responsive PD-nanoparticles are retained in the tumor. Therapeutic application of PD labeled with beta- or alpha-emitting radionuclides can be expected.

4. CELL TRAFFICKING

4.1 Light-Emitting Bacteria to Target Tumor [7]

Cancer researchers have long sought a magic bullet that would selectively target malignant cells. There has been a long history of reports over 60 years that bacteria can selectively grow in tumors. We exploited the fact that E. coli injected into tumor-bearing mice selectively target and proliferate in solid tumors in vivo by employing genetically engineered bioluminescent E. coli and optical molecular imaging techniques.

pUC19 plasmid encloning *Lux* or GFP, bioluminescent or fluorescent reporter gene, was transformed into wild type (MG1655) or mutant *E.* coli strains. For stably expressing *lux*, *lux* was cloned with asd (aspartate β-semialdehyde dehydrogenase) gene and transformed into asd defective *E. coli* (MG1655asd-/asd$^+$*lux*) that would prevent *E. coli* from releasing lux plasmid inside the tumor cells. These bacteria were i.v. or i.p. injected into tumor mice (CT26, C6, MCF-7, B16F10, ARO). The imaging signal from MG 1655*lux* was detected initially in the liver (20min), and thereafter at tumors for at least 1 week in both nude and Balb/c mice. MG1655asd$^-$/asd$^+$*lux* produced stronger and longer-lasting (for 2 weeks) signal from tumor than did MG 1655*lux*. Directly injected MG1655asd$^-$/asd$^+$*lux* was transiently observed in central necrosis regions. It then spreaded to the peripheral proliferative area. Flagella-defective (FlhD$^-$) and aerotaxis-defective (Aer$^-$) mutants completely failed to reach the tumor loci. Regulatory mutants defective in

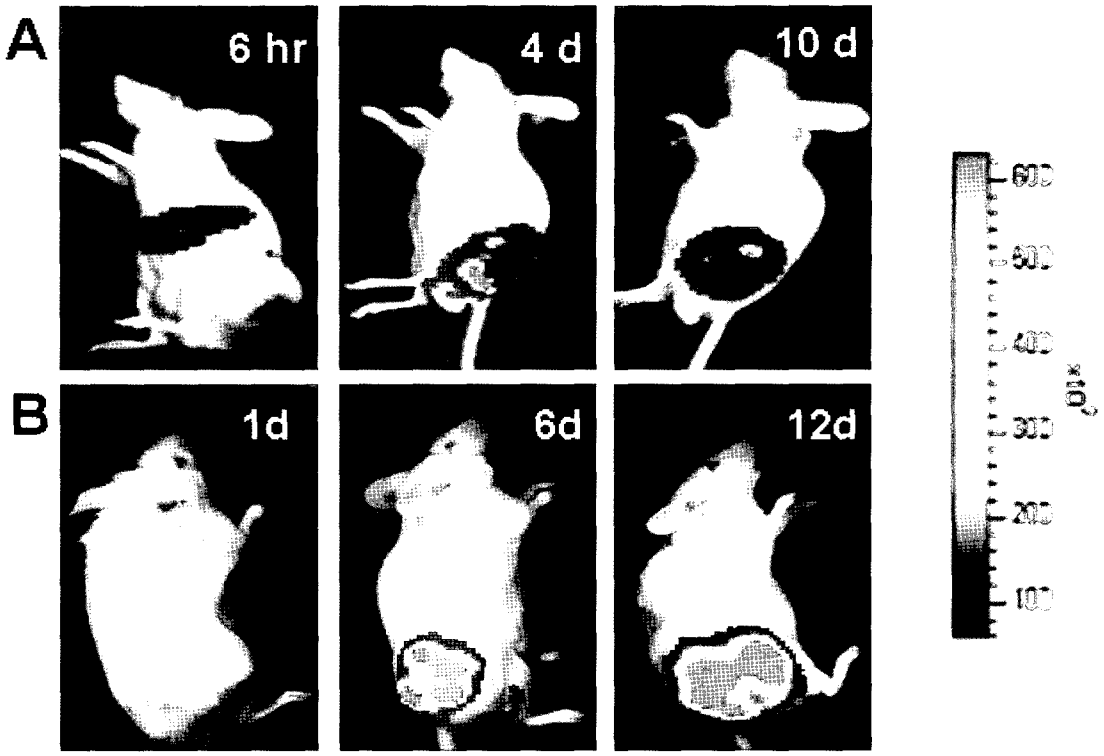

Fig. 3. Bioluminescence Imaging of Cancer Cells by Using Genetically Engineered Light-emitting Bacteria. Lux-expressing Bacteria Successfully Target Tumor Tissues in Nude (A) and Balb/c (B) Mouse

sensing environmental stress (ppGpp$^-$, rpoS$^-$) couldn't reach and proliferate in tumor. Directly injected FlhD$^-$ strains into tumor necrotic portion just stayed there and did not proliferate to adjacent area in tumors.

E. coli strongly targeted solid tumors regardless of host's immune status. Our results support that the targeting of tumor by *E. coli* is an active process, with flagella function and the mechanism would be possibly related to aerotaxis. Live attenuated *E. coli* could be applied as a delivery vehicle of varying imaging markers or therapeutic molecules. Fig. 3 is the bioluminescence imaging of cancer cells by using genetically engineered light-emitting bacteria.

4.2 Dendritic Cell Trafficking [8]

The purpose of this study was to evaluate the migration of technetium-99m hexamethyl propylene amine oxime (^{99m}Tc-HMPAO) labeled immature and mature dendritic cells (DC) in the mouse. DC were collected from bone marrow (BM) of tibiae and femurs of mice. Immature and mature DC from BM cells were radiolabeled with ^{99m}Tc-HMPAO. To evaluate the functional and phenotypic changes of DC from radiolabeling, the allogeneic mixed lymphocte reaction (MLR) and fluorescence-activated cell sorting (FACS) analysis were performed before and after labeling with ^{99m}Tc-HMPAO. Migration of *intravenously* injected DC (iv-DC) was assessed by serial gamma camera imaging of mice with or without subcutaneous tumors. Percent injected dose per gram (%ID/g) was calculated in lungs, liver, spleen, kidneys and tumor through dissection of each mice after 24 hours of injection. Labeling efficiency of immature and mature DC were 60.4±5.4% and 61.8±6.7%, respectively. Iv-DC initially appeared in the lungs, then redistributed mainly to liver and spleen. Migration of mature DC to spleen was signficantly higher than immature DC (38.3±4.0 % vs. 32.2±4.1 % in control group, 40.4±4.1% vs. 35.9±3.8 % in tumor group; $p<0.05$). Migration to tumor was also significantly higher in mature DC than in immature DC (2.4±0.3% vs 1.7±0.2%; $p=0.034$). In conclusion, assessment of migration pattern of DC in mice was possible using ^{99m}Tc-HMPAO labeled immature and mature DC. Migration of mature DC to spleen and tumor was higher than that of immature DC when they were *i.v.* injected.

4.3 Stem Cell Trafficking [9]

The conventional method of analyzing myocardial cell transplanation relies on postmortem histology. We sought to demonstrate the feasibility of longitudinal monitoring transplanted cell survival in living animals using optical

imaging techniques. Umblical cord blood was collected upon delivery with informed consent. Umblical mononuclear cells were obtained by negative immuno-depletion of CD3, CD14, CD19, CD38, CD66b and glycophorin-A positive cells, followed by Ficoll-Paque density gradient centrifugation, and plated in non-coated tissue culture flasks in expansion medium. Cells were allowed to adhere overnight; thereafter non-adherent cells were washed out with medium changes. After obtaining the MSCs, they were transfected [multiplicity of infection (MOI) = 40] with Ad-CMV-Fluc overnight. Rats (n=4) underwent intramyocardial injection of 5×10^5 MSCs expressing the firefly luciferase (Fluc) reporter gene. Optical bioluminescence imaging was performed using the charged-coupled device camera (Xenogen) from the first day of transplantion. Cardiac bioluminescence signals were present from second day of transplantation. Cardiac signals were clearly present at day 2 (9.2×10^3 p/s/cm^2/sr). The signal reduced from day 3. In conclusion, the locations, magnitude, and survival duration of cord-blood-derived MSCs were monitored noninvasively. With further development, molecular imaging studies should add critical insights into cardiac cell transplantation.

5. CONCLUSIONS AND FUTURE PERSPECTIVES

Molecular imaging strategies will likely expand significantly over the next few years as imaging and molecular genetic technologies continue to evolve. The explosion in genetic engineering is expected to generate more robust gene transfer vectors, both viral and non-viral. Optical technologies including fluorescence tomography may allow optical strategies to be the method of choice for small animal research. These strategies will spread into PET, MRI or CT studies. Multimodality reporter gene approaches will permit investigators to readily move between the various technologies and should help to study various pre-clinical models. This potential power of molecular imaging to see fundamental biological processes in a new light will not only help to enhance our overall knowledge and understanding but should also accelerate considerably the rate of discovery in the biological sciences.

REFERENCES

[1] E.M. Kim, H.J. Jeong, I.K. Park, C.S. Cho, C.G. Kim and H.S. Bom, "Hepatocyte-Targeted Nuclear Imaging Using ^{99m}Tc-Galactosylated Chitosan: Conjugation, Targeting, And Biodistribution," *J. Nucl. Med.* **46**, 141 (2005).

[2] E.M. Kim, H.J. Jeong, I.K. Park, C.S. Cho, H.S. Bom and C.G. Kim, "Monitoring the Effect of Pegylation on Polyethylenimine In Vivo Using a Nuclear Imaging Technique," *Nucl. Med. Biol.* **31**, 781 (2004).

[3] E.M. Kim, H.J. Jeong, I.K. Park, C.S. Cho, H.B. Moon, D.Y. Yu, H.S. Bom, M.H. Sohn and I.J. Oh, "Asialoglycoprotein Receptor Targeted Gene Delivery Using Galactosylated Polyethylenimine-Graft-Poly (Ethylene Glycol): In Vitro And In Vivo Studies," *J. Control. Release.* **108**, 557 (2005).

[4] C.M. Lee, Y.D. Choi, E.J. Huh, K.Y. Lee, H.C. Song, M.J. Sun, H.J. Jeong, C.S. Cho and H.S. Bom, "Polyethylene Glycol (PEG) Modified ^{99m}Tc-HMPAO-Liposome For Improving Blood Circulation And Biodistribution: The Effect Of The Extent Of Pegylation," *Cancer Biother. Radiopharm.* In press.

[5] S.M. Kim, H.S. Bom, H.J. Jeong, H.C. Song, E.M. Kim, Y.J. Heo, J.W. Lee, C.K. Kim, M.H. Li and H.K. Ro, "Comparison of Images With ^{99m}Tc-transferrin and ^{67}Ga-citrate in a Rat Abscess Model," *J. Nucl. Med.* **45**, 298P (2004).

[6] H.C. Song, H.S. Bom, K. Na, K.Y. Lee, Y.J. Heo and S.M. Kim, "Biodegradable Nano-Sized Pullulan Derivatives for Tumor-Targeted Delivery of Radioisotopes," *J. Nucl. Med.* **44**, 303P (2003).

[7] H.S. Bom, "Bioluminescent optical imaging," *Proc. Korean Soc. Mol. Imaging.* (2004).

[8] M.H. Li, H.S. Bom, H.C. Song, Y.J. Heo and J.J. Lee, "Migration of Tc-99m-HMPAO Labeled Immature and Mature Dendritic Cells in the Mouse," *J. Nucl. Med.* **45**, 489P (2004).

[9] J.J. Min, Y.K. Ahn, S.M. Moon, S.Y. Lim, K.H. Yun, Y.J. Heo, H.C. Song, M.H. Jeong and H.S. Bom, "Bioluminescence Imaging of Cord Blood Derived Mesenchymal Stem Cell E. coli Transplanatation into Myocardium," *Kor. J. Nucl. Med.* **38**, 388 (2004).